BIOCHEMISTRY
including biophysical chemistry & molecular biology

Article

Investigation of the binding interaction of fatty acids with human G protein coupled receptor 40 using a site-specific fluorescence probe by flow cytometry

Xiao-Min Ren, Linying Cao, Jing Zhang, Wei-Ping Qin, Yu Yang, Bin Wan, and Liang-Hong Guo

Biochemistry, **Just Accepted Manuscript** • DOI: 10.1021/acs.biochem.6b00079 • Publication Date (Web): 14 Mar 2016

ACS Publications

Biochemistry is published by the American Chemical Society. 1155 Sixteenth Street N.W., Washington, DC 20036

Investigation of the binding interaction of fatty acids with human G protein coupled receptor 40 using a site-specific fluorescence probe by flow cytometry

Xiao-Min Ren[1], Lin-Ying Cao[1], Jing Zhang[1], Wei-Ping Qin[3], Yu Yang[1], Bin Wan[1], Liang-Hong Guo[1,2*]

1. State Key Laboratory of Environmental Chemistry and Eco-toxicology, Research Center for Eco-environmental Sciences, Chinese Academy of Sciences, 18 Shuangqing Road, P.O. Box 2871, Beijing, 100085, China

2. Institute of Environment and Health, Jianghan University, Wuhan, 430056, China

3. College of Life and Environmental Science, Minzu University of China, Beijing, 100081, China

Corresponding author

*Liang-Hong Guo, State Key Laboratory of Environmental Chemistry and Eco-toxicology, Research Center for Eco-environmental Sciences, Chinese Academy of Sciences, 18 Shuangqing Road, P.O. Box 2871, Beijing, 100085, China

Phone & Fax: +86 10-62849685

E-mail: LHGuo@rcees.ac.cn

Funding Source Statement

This work was supported by the Chinese Academy of Sciences (XDB14040100) and National Natural Science Foundation of China (21321004, 21375143, 91543203, 21407168, 21377142 and 21477146).

Abbreviations

human G protein coupled receptor 40 (hGPR40)

free fatty acids (FFAs)

fluorescein-TAK-875 analogue (F-TAK-875A)

human embryonic kidney (HEK)

flow cytometry (FCM)

Abstract

Human G protein coupled receptor 40 (hGPR40), with medium- and long-chain free fatty acids (FFAs) as its natural ligands, plays an important role in the enhancement of glucose-dependent insulin secretion. To date, information about the direct binding of FFAs to hGPR40 is very limited and how carbon chain length affects the activities of FFAs on hGPR40 is not yet understood. In this study, a fluorescein-fasiglifam analogue (F-TAK-875A) conjugate was designed and synthesized as a site-specific fluorescence probe to study the interaction of FFAs with hGPR40. The hGPR40 was expressed in human embryonic kidney 293 cells and labeled with F-TAK-875A. By using flow cytometry, competitive binding between FFA and F-TAK-875A to hGPR40 expressed cells was measured. Binding affinities of 18 saturated FFAs, with carbon (C) chain lengths ranging from C6 to C23, were analyzed. The results showed that the binding potencies of FFAs to hGPR40 were carbon length-dependent. There was a positive correlation between length and binding potency for 7 FFAs (C9 to C15), with myristic acid (C15) showing the highest potency, 0.2% relative to TAK-875. For FFAs with length less than C9 or more than C15, they had very weak or no binding. Molecular docking results showed that the binding pocket of TAK-875 in hGPR40 could enclose FFAs with lengths of C15 or fewer. However, for FFAs with lengths longer than C15, part of the alkyl chain extended out of the binding pocket. This study provided insights into the structural dependence of FFAs binding to and activation of hGPR40.

The human G protein coupled receptor 40 (hGPR40), also known as free fatty acid receptor 1, is highly expressed in humans in pancreatic β cells, brain and endocrine cells of the gastrointestinal tract.[1-3] Free fatty acids (FFAs), which are essential nutritional components, were identified as the natural substrates of GPR40.[4, 5] Medium- and long-chain FFAs activated Gq coupled GPR40 leading to activation of phospholipase C and subsequent elevation of intracellular Ca^{2+}.[6, 7] Several *in vitro* and *in vivo* studies have demonstrated that FFAs augmented glucose-stimulated insulin secretion in pancreatic β cells by specifically activating GPR40.[8, 9] Therefore, GPR40 is regarded as an attractive target for enhancing insulin secretion in patients with type 2 diabetes.[10, 11] Many potent GPR40 ligands, such as fasiglifam (TAK-875), GW9508 and AMG 837, have been synthesized as potential drugs.[12-18]

To date, most studies of activation of chemicals on GPR40, including activation of FFAs and synthetic chemicals, involved monitoring GPR40-mediated cellular Ca^{2+} mobilization.[1, 19] For example, Itoh *et al*. compared activities of nine saturated FFAs, with carbon chain (C) length ranging from C2 to C18, in hGRP40 expressing Chinese hamster ovary cells. FFAs with carbon lengths shorter than C8 had no agonist activity. Activity increased when the length increased from C8 to C16, but decreased as length increased further from C16 to C18. FFAs with C12, C14 and C16 had similar activities.[20] Briscoe *et al*. studied the activities of 18 saturated FFAs (C6−C23) in hGRP40 expressing human embryonic kidney (HEK) 293 cells. They found that activity increased with FFA length from C6 to C16, but decreased as carbon length increased from C17 to C23. No activity was found for the FFA with lengths shorter than C6.[21] GPR40 activation by FFAs was found to be related to their carbon chain length. However, the underlying mechanism regulating the effect of FFA carbon length on GPR40 activation remains to be elucidated.

To study the pharmacology of ligands on GPR40 more directly, a quantitative method to evaluate binding potency is needed. Direct binding assays for GPR40 have required development of specific labeled probes. Hara *et al*. showed that fluorescently labeled FFAs, such as C1-BODIPY-C12, could specifically bind to GPR40.[22] By

measuring the amount of C1-BODIPY-C12 bound to GPR40 immobilized beads with flow cytometry, they studied the binding potencies of sixteen ligands (including ten FFAs, troglitazone, pioglitazone, rosiglitazone, ciglitazone, MEDICA16 and GW9508) to GPR40. In another study, Lin *et al*. synthesized two radioligands, [^{3}H]AMG 837 and [^{3}H]AM 1638.[23] Competitive binding of five chemicals (docosahexaenoic acid, AMG 837, AM 1638, AM 6331 and AM 8182) with the radioligands to GPR40 on isolated cell membranes revealed their receptor binding properties. Hauge *et al*. also compared the binding properties of a series of GPR40 agonists (including 2 FFAs, TAK-875, MK-2305, AM-8182, AM-1638, AM-5262) by using the radioligands [^{3}H]AM 1638 and [^{3}H]L358.[24] In addition, a liquid chromatography–mass spectroscopy (LC–MS) based ligand binding assay was described investigating the binding potency of TAK-875 to GPR40 on isolated membranes.[25]

In this study, we designed and synthesized a site-specific fluorescence probe for hGPR40. Informed by crystal structure data on hGPR40 bound to TAK-875 and structure-activity relationship data obtained for TAK-875 analogues,[14, 25, 26] we conjugated a TAK-875 analogue with a fluorescein group to make it a potential fluorescence probe. We also established a flow cytometry (FCM)-based competitive binding assay to monitor the interaction of ligands with hGPR40 expressed in HEK 293 cells. Using these tools and methods, we evaluated the binding potencies of 18 saturated FFAs with hGPR40, examining effects of carbon chain length on binding affinity. To further understand the mechanism of FFA binding affinity and activation of hGPR40, we employed molecular docking to investigate the interaction of FFAs with the receptor.

Materials and Methods

Chemicals

TAK-875 was from Selleckchem (Figure 1). GW9508 and the 18 FFAs (Figure 1) were from Sigma Aldrich (St. Louis, MO, USA). The 18 FFAs were: n-caproic acid ($C_6H_{12}O_2$), heptanoic acid ($C_7H_{14}O_2$), caprylic acid ($C_8H_{16}O_2$), nonanoic acid ($C_9H_{18}O_2$), capric acid ($C_{10}H_{20}O_2$), undecanoic acid ($C_{11}H_{22}O_2$), lauric acid

($C_{12}H_{24}O_2$), tridecanoic acid ($C_{13}H_{26}O_2$), myristic acid ($C_{14}H_{28}O_2$), pentadecanoic acid ($C_{15}H_{30}O_2$), palmitic acid ($C_{16}H_{32}O_2$), heptadecanoic acid ($C_{17}H_{34}O_2$), stearic acid ($C_{18}H_{36}O_2$), nonadecanoic acid ($C_{19}H_{38}O_2$), arachidic acid ($C_{20}H_{40}O_2$), heneicosanoic acid ($C_{21}H_{42}O_2$), behenic acid ($C_{22}H_{44}O_2$), and tricosanoic acid ($C_{23}H_{46}O_2$). FFA stock solutions were prepared by dissolving the FFA in dimethyl sulfoxide (DMSO) at concentrations from 1–100 mM, depending on solubility. All other reagents were of the highest available purity.

Fluorescence probe synthesis

We synthesized a fluorescein-TAK-875 analogue (F-TAK-875A) conjugate as outlined in Scheme 1 (Figure S1). From the results of hGPR40/TAK-875 crystal structure and the findings on the structure-activity relationship of TAK-875 analogues, the 4′-position of the terminal biphenyl ring was found to tolerate a variety of modifications with minimal effect on binding potency and the sulfonate group of TAK-875 was not required for its agonist activity.[14, 25, 26] Thus, we designed a TAK-875 analogue by replacing the 3-(methylsulfonyl)propoxy moiety of TAK-875 with a 3-(amino)ethyoxyl, and reacting this analogue with the 5(6)-carboxy fluorescein succinimidyl ester (NHS-fluorescein) (Life Technologies, Carlsbad, CA, USA) (Figure1 and Figure S1). Unlike TAK-875, which is an (S)-enantiomer, the TAK-875 analogue we synthesized was a racemic mixture (Figure1). The synthesis and characterization of F-TAK-875A is detailed in the Supplementary Materials and Methods. The synthetic product (with purity >98%, Figure S2) had the correct molecular weight of 806.7 $(M+H)^+$ (Figure S3). Proton nuclear magnetic resonance (^{1}H NMR) results were consistent with the correct structure of F-TAK-875A (Figure S4). F-TAK-875A stock solution, at a concentration of 100 μM, was prepared in DMSO. The concentration of the probe was determined by absorbance at 490 nm, using a molar extinction coefficient of 7.8×10^4 $M^{-1}cm^{-1}$.

Cell culture and plasmid construction

HEK 293 cells (American Type Culture Collection, Manassas, VA, USA) were cultured in Dulbecco's modified Eagle's medium (DMEM) (Life Technologies)

supplemented with 10% fetal bovine serum (Life Technologies), penicillin (100 units/mL) and streptomycin (100 mg/mL) (Life Technologies) at 37 °C in a humidified incubator equilibrated with 5% CO_2, 95% air. All cells used in our experiments were at the exponential growth phase.

Two hGPR40 expression plasmids, hGPR40-FLAG and hGPR40-enhanced green fluorescent protein (EGFP), were constructed by GeneChem (Shanghai, China). Cloning of the hGPR40 (GenBank accession number BC120944) from human genomic DNA was performed by PCR using the following primers (hGPR40–FLAG plasmid, forward: 5′-ACGGGCCCTCTAGACTCGAGCGCCACCATGGACCTGCCCCCGCAGCTC-3′ reverse: 5′-AGTCACTTAAGCTTGGTACCGACTTCTGGGACTTGCCCCCTTG-3′; hGPR40-EGFP plasmid, forward: 5′-TACCGGACTCAGATCTCGAGATGGACCTGCCCCCGCAGCTC-3′; reverse: 5′-GATCCCGGGCCCGCGGTACCGTCTTCTGGGACTTGCCCCCTTG-3′). The PCR products were restricted with XhoI/KpnI, subcloned into the GV141 vector (GeneChem) to obtain hGPR40-FLAG, with XhoI/KpnI, subcloned into the GV143 vector (GeneChem) to obtain hGPR40-EGFP, respectively. FLAG and EGFP control plasmids were all purchased from GeneChem.

FCM analysis

HEK 293 cells were seeded in 100-mm dishes (Corning, NY, USA) at 5×10^6 cells per dish to obtain 70–80% confluence. On the next day, the medium was changed to phenol red-free DMEM (Life Technologies) with 10% charcoal dextran-treated fetal bovine serum (HyClone, Logan, UT, USA). Cells (in 5 mL medium) were then transfected with 8 μg plasmids using a lipofectamine 2000 transfection reagent (Life Technologies) at a 1:2.5 ratio according to the manufacturer's instructions. After 48 h, cells were harvested by trypsin-EDTA (Life Technologies), washed twice in ice-cold phenol red-free DMEM and placed on ice in 5 mL phenol red-free DMEM. For the FCM assay, cell samples were prepared by

suspended 50 μL harvested cells (approximately 1×10^5 cells) in 450 μL phosphate-buffered saline (PBS) buffer (137 mM NaCl, 2.7 mM KCl, 10 mM Na_2HPO4, 1.8 mM KH_2PO_4 pH 7.4) in a total volume of 500 μL. Cell samples were analyzed in a NovoCyte Flow Cytometer (ACEA Biosciences, CA, USA). At least 10,000 events were analyzed per sample, using forward scatter versus side scatter dot-plot gating to resolve the primary population of cells. The fluorescence intensity of cells in the fluorescein isothiocyanate (FITC) channel for each sample was recorded in log mode.

FCM-based hGPR40 binding assay

For saturation binding analysis, 50 μL hGPR40-FLAG transfected HEK 293 cells (hGPR40 cells) (approximately 1×10^5 cells) were incubated in PBS buffer with increasing concentrations of F-TAK-875A in a total volume of 500 μL. Reactions were incubated at room temperature for 2 min, which is sufficient for binding (Figure S5). Non-specific binding was determined using control incubations measuring binding of F-TAK-875A with FLAG transfected HEK 293 cells (FLAG cells) and binding of unconjugated FITC with hGPR40 cells. The percentage of F-TAK-875A bound hGPR40 cells to total number of hGPR40 cells was plotted as a function of probe concentration to obtain the saturation curve, which was fitted by nonlinear regression (GraphPad Prism, La Jolla, CA, USA).

In competitive binding assays, 50 μL hGPR40 cells (approximately 1×10^5 cells), 100 nM F-TAK-875A and diluted test molecules were mixed in PBS in a total volume of 500 μL and incubated for 2 min at room temperature. The percentage of F-TAK-875A bound hGPR40 cells to total number of hGPR40 cells was plotted as a function of ligand concentration to obtain the competition curve. The competition curve for each ligand was fitted with a sigmoidal model (OriginLab, Northampton, MA, USA) to calculate the IC_{50}. Relative binding potency (RP), in comparison with that of TAK-875 (binding potency set to 1), was obtained by dividing the IC_{50} of TAK-875 by that of the other chemical. The test compounds had no effect on non-specific binding of F-TAK-875A to FLAG cells at the highest tested

concentrations (Figure S6). The final concentration of DMSO in the assay was 1%, which had no effect on the binding of F-TAK-875A to hGPR40 cells (Figure S7).

Molecular docking

AutoDock 4.2 (La Jolla, CA, USA) was used to simulate interactions between ligands and hGPR40. The crystal structure of hGPR40 (PDB ID 4PHU) was extracted from the RCSB Protein Data Bank (http://www.rcsb.org/pdb). The 3-dimensional coordinates of the ligands in the PDB format were obtained through the PRODRG server.[27] When docking, the hGPR40 was kept rigid, while all torsional bonds of each ligand were set as free. A pre-calculated 3-dimensional energy grid of equally spaced discrete points was generated prior to docking for a rapid energy evaluation, using the program AutoGrid. The grid box, with dimensions of 80×80×60 Å, was centered at the TAK-875 binding site of the hGPR40 molecule and covered the entire binding site and its neighboring residues. The distance between two grid points was set to 0.375 Å. Docking was performed using the Lamarckian genetic algorithm. Ten independent docking runs were conducted for each complex and the binding mode with the lowest binding energy was selected for further analysis.

Statistical analysis

The *p* values of the experimental data were each determined by two-way ANOVA followed by Duncan post hoc analysis. A *p* value of less than 0.05 was considered statistically significant. All experiments were conducted in triplicate (n=3) and the data were expressed as the means±standard deviation (SD).

Results

Expression of hGPR40 in HEK 293 cells

To ensure positive expression of hGPR40 in HEK 293 cells, a vector containing hGPR40 fused with EGFP at the C-terminus was constructed and transiently expressed in the cells (hGPR40-EGFP cells). With this vector, expression of hGPR40-EGFP should give a strong FITC signal. As shown in Figure 2A, the background FITC signal in cells was distributed in region A. For hGPR40-EGFP cells, some cells had stronger FITC signal in region B, indicating expression of

hGPR40-EGFP (Figure 2B). The results showed that hGPR40 was expressed in the HEK 293 cells. The hGPR40-FLAG construction was then used for further development of the hGPR40 binding assay.

Specific binding of F-TAK-875A to hGPR40

The F-TAK-875A conjugate was designed and synthesized as a potential fluorescence probe for hGPR40 binding. It was anticipated that the TAK-875A moiety of the conjugate would provide site-specific binding to hGPR40 and that the FITC group would serve as a signal reporter. To demonstrate the probe binding to hGPR40, we investigated the interaction of F-TAK-875A with hGPR40-FLAG transfected HEK 293 cells (hGPR40 cells) by FCM. After incubating cells with F-TAK-875A, the mean value and histogram distribution of FITC signals of cells were determined.

The F-TAK-875A might bind to cells through both specific binding to hGPR40 and non-specific binding to other cellular regions. Cells binding more F-TAK-875A would have stronger FITC signals. As shown in Figure 3A and B, hGPR40 cells had higher FITC signals than FLAG cells at various probe concentrations, suggesting that hGPR40 cells bound more F-TAK-875A. The additional FITC signal observed with hGPR40 cells should represent specific binding of F-TAK-875A to the receptor. Because HEK 293 cells were transient transfected with plasmids, only some of the cells expressed the foreign protein (Figure 2B). As shown in Figure 3C, after incubation with F-TAK-875A, the FITC signals from the FLAG cell sample exhibited a normal distribution, with 96.2% and 2.1% percent of cells distributed in regions A and B, respectively. However, those from the hGPR40 cell sample did not exhibit a normal distribution. Besides the peak distributed in region A, it had an additional peak distributed in region B (comprising 12.5% of cells) (Figure 3C). We assumed that only the hGPR40 expressing [$hGPR40^{(+)}$] cells could specifically bind with F-TAK-875A, showing a higher FITC signals than cells with negative expression [$hGPR40^{(-)}$]. Thus, we inferred that the signals distributed in regions A and B represented F-TAK-875A bound $hGPR40^{(-)}$ and $hGPR40^{(+)}$ cells, respectively. To confirm this, we used TAK-875 to compete with F-TAK-875A binding to $hGPR40^{(+)}$

cells. As shown in Figure 3C, the addition of TAK-875 completely eliminated the additional peak, leaving only 2.3% percent of cells distributed in region B. The above results demonstrated that F-TAK-875A could bind to hGPR40 specifically. The percentage of probe bound hGPR40$^{(+)}$ cells in total number of hGPR40 cells could be used to indicate the interaction of F-TAK-875A with hGPR40.

To establish a competitive binding assay, the binding constant of the probe (F-TAK-875A) for the target protein (hGPR40) needed to be determined. Using the percentage of cells distributed in region B to indicate specific binding of F-TAK-875A to hGPR40, we performed saturation experiments (Figure 3D). The percentage of cells distributed in region B increased significantly (p<0.05) from 2.1% to 10.2% with increasing concentrations of F-TAK-875A, reflecting binding of F-TAK-875A to hGPR40. No such concentration-dependent increase was observed with F-TAK-875A in FLAG cells. In another control experiment, no such increase was found with FITC in hGPR40 cells (Figure 3D). From the saturation curve, an apparent equilibrium dissociation constant (K_d) of 15.1±3.2 nM was determined for binding of F-TAK-875A to hGPR40.

Binding affinity of TAK-875, GW9508 and 18 saturated FFAs to hGPR40

The binding potencies of 18 saturated FFAs, with carbon chain lengths from C6 to C23, to hGPR40 were assessed quantitatively by the FCM-based competitive binding assay. TAK-875 and GW9508, two known potent ligands for hGPR40, were used as positive controls. A series of ligand concentrations were added to mixtures with F-TAK-875A and hGPR40 cells. As the ligand concentrations increased, more F-TAK-875A was displaced from hGPR40$^{(+)}$ cells, leading to a decreased percent of F-TAK-875A labeled cells. The competition curves obtained with all compounds are shown in Figure 4 and Figure S8. From these curves, IC_{50} and RP values for the ligands were calculated and are listed in Table 1. As shown in Figure 4A and B, both TAK-875 and GW9508 completely inhibited F-TAK-875A binding, with IC_{50} values of 3.1±0.8 and 25.1±2.8 nM, respectively. Based on the competitive binding assays, the hGPR40 binding potency of the 18 saturated FFAs varied significantly, with

myristic acid (C15 FFA) showing the greatest potency at 0.2% relative to TAK-875 (binding potency set to 1). For three short-chain saturated FFAs (C6–C8), no hGPR40 binding was found even at the highest concentration (1000 μM). For the seven medium- and long-chain saturated FFAs (C9–C15), RP increased with carbon length from 3.1×10^{-8} for C9 to 2.1×10^{-3} for C15. However, a decreased binding potency was observed with palmitic acid (C16 FFA), which bound to hGPR40 cells so weakly that its IC_{50} could not be obtained at the highest concentration (10 μM, solubility prevented higher concentrations from being tested). For the other seven long-chain saturated FFAs (C16–C23), no hGPR40 binding was found even at the highest concentration (10 μM, solubility prevented higher concentrations from being tested).

Molecular docking of TAK-875, GW9508 and 18 FFAs with hGPR40

From the competitive binding results, we determined that the 18 tested FFAs, with very similar chemical structures and differing only in carbon chain length, had very different binding affinities for hGPR40. To reveal the structural basis for these differences in binding potency, we used molecular docking analysis to provide insights into the interactions between FFAs and hGPR40. The 18 FFAs were docked into the TAK-875 binding pocket of hGPR40. In addition, TAK-875 and GW9508 were also included in the docking analysis for comparison. The structures of the docked hGPR40/ligand complexes are shown in Figure 5 and Figure S8. The results of hydrogen bond interactions with hGPR40 obtained for all chemicals are listed in the Table 1.

A previous crystal structure study revealed that TAK-875 bound to hGPR40 with its carboxylic acid end forming hydrogen interactions with several hydrophilic amino acids in the inner part of the binding pocket and its hydrophobic moiety situated between transmembrane helixes 3 and 4.[25, 28] Presumably, the binding pocket of TAK-875 in hGPR40 can be subdivided into two regions, a hydrophilic portion interacting with the carboxylic acid substituent and an outer hydrophobic portion contacting the hydrophobic moiety of TAK-875. As shown in Figure 5A, TAK-875 docked into hGPR40 with the predicted orientation, with its carboxylic acid

substituent locating at the inner part and its methylsulfonyl located towards the entrance of the binding pocket. The hydrogen bonding interactions observed between TAK-875 and Arginine (Arg) 183, tyrosine (Try) 2240 and Arg 2258 are consistent with previous crystal structure results.[25] GW9508 docked into hGPR40 with a similar mode as TAK-875, with its carboxylic acid substituent locating at the inner part, forming hydrogen bonding interactions with Arg 183 and Arg 2258 (Figure 5B).

The 18 saturated FFAs had similar structures composed of two parts, a carboxylic acid end and an alkyl chain, the latter of various lengths. Docking results indicated that all FFAs could fit into the TAK-875 binding pocket of hGPR40. They had similar binding modes to that of TAK-875, with their acid end group located at the inner part and the hydrophobic alkyl chain toward the entrance of the binding pocket (Figures 5C–F and Figure S8). The hydrogen bonding interactions observed between FFAs and hGPR40 were also similar as with TAK-875. All the FFAs could form hydrogen bonds with Arg 183 and Arg 2258 (Table 1). Of the 18 FFAs, 11 could form hydrogen bonds with Tyr 2240 (Table 1).

Discussion

In this study, we designed and synthesized a site-specific fluorescence probe, F-TAK-875A, to study the interaction of FFAs with hGPR40. The results of a FCM-based binding assay suggested that F-TAK-875A could specifically bind to hGPR40 expressed on HEK 293 cells. Using this probe, we established a FCM-based competitive binding assay to monitor the interaction of FFAs with hGPR40. Several methods have been previously employed to study the direct binding of ligands to GPR40.[22, 23, 25] The FCM-based competitive binding assay established in our study had several advantages compared with these other methods. The probe was designed by conjugating a FITC group to TAK-875A, so was expected to bind to hGPR40 at the same site as this parent ligand. Thus, with the site-specific probe F-TAK-875A, we were able to measure the potency of ligand binding to hGPR40 specifically at the TAK-875 binding site. In addition, in contrast to previous methods using isolated GPR40-expressing cell membranes or immunopurified receptor, we studied the

binding of ligands to hGPR40 expressed in the membranes of living cells, more closely maintaining the natural state of the receptor. Furthermore, this FCM-based competitive binding assay did not require separation of free and bound ligands, making it potentially useful for high-throughput screening for hGPR40 ligands.

Using the established method, we first compared the binding potency of GW9508 with that of TAK-875. Our results showed that the binding potency of TAK-875 to hGPR40 was 8.1 times higher than that of GW9508, which is in consistent with the results of agonist activities of them obtained by GPR40-mediated cellular Ca^{2+} mobilization, that the agonist activity of TAK-875 was 1.6 times greater than that of GW9508.[13] Furthermore, we determined the binding potencies of 18 FFAs with hGPR40 to obtain some structural information about FFA binding. With the site-specific probe F-TAK-875A, we demonstrated that FFAs bound to hGPR40 specifically at the TAK-875 binding site. With the large number of FFAs tested in our study, a clear trend linking structure to binding potency emerged. That is, hGPR40 binding potency was associated with FFA carbon chain length. For FFAs with carbon chain lengths in the range of C9 to C15, a positive correlation between RP and chain length (R^2=0.89) was observed. For FFAs with carbon chain lengths of less than C9 or more than C15, very weak or no receptor binding was observed at tested concentrations. Previous data describing direct binding of FFAs to GPR40 is very limited. To our knowledge, only one paper described binding of FFAs to hGPR40 using a FCM based assay. That study tested only three saturated FFAs, and their binding potencies were in the order of palmitic acid (C16)> lauric acid (C12) > capric acid (C8).[22] In contrast, our data showed that the binding potency of palmitic acid (C16) was lower than that of lauric acid (C12). This inconsistency between studies might be caused by the use of different probes or by differences in the state of the hGPR40.

To date, most of the studies on FFA-dependent activation of GPR40 were obtained by measuring GPR40-mediated cellular Ca^{2+} mobilization in GRP40 expressing cells.[1, 2, 14, 19] GPR40 activation by FFAs was found to be related to the

carbon chain length, with medium- and long-chain FFA had highest agonist activity. Compared with the results of Ca^{2+} mobilization in previous studies, our binding results correlated well with the agonist activities of FFAs. The medium- and long-chain FFAs were found to be with higher binding affinity to hGPR40 than other FFAs. Because ligand activation of a receptor depends primarily on its binding affinity, we speculate that the activities of FFAs at hGPR40 might be determined by their binding affinities.

Molecular docking analysis was performed between FFAs and hGPR40 so as to provide some information about the structural characteristics of the ligand binding to and agonistic activity of hGPR40. These results indicated that all FFAs could fit into the TAK-875 binding pocket of hGPR40 with their carboxylic acid ends forming hydrogen interactions on the inside and the alkyl chains situated at the same place as the hydrophobic moiety of receptor-bound TAK-875. However, the exact binding geometry was slightly different among FFAs of various carbon chain lengths. The FFAs with lengths shorter than C15 bound to hGPR40 inside the binding core of the receptor for TAK-875 (Figure 5 C–E and G and Figure S8). However, the FFAs with lengths longer than C15 had molecular sizes that were too big for the binding pocket. They could not be enclosed in the core of the binding site of TAK-875 and thus utilized a different binding mode. The acid end group and neighboring alkyl moiety of a long-chain FFA occupied the binding core fully, with the rest of the alkyl chain extending outside the binding pocket (Figure 5 F and H and Figure S8). We speculated, therefore, that for the FFAs with carbon chain lengths shorter than C15, as the carbon number increased, their hydrophobicity also increased. This led to stronger hydrophobic interactions with the protein. The positive correlation between hGPR40 binding affinity and carbon chain length observed in the current study can be explained by the molecular docking results. For FFAs with carbon lengths greater than C15, their molecular sizes are larger than the volume of the TAK-875 binding pocket. In this case part of the alkyl chains, which are highly hydrophobic, extended out of the binding pocket. This might destabilize the binding between FFAs and

hGPR40. Overall, the docking results appeared to explain our observed FFA binding potency data well.

Conclusion

In this study, a site-specific hGPR40 fluorescence probe, F-TAK-875A, was designed and synthesized. The TAK-875A moiety of this probe could bind specifically to hGPR40 at the TAK-875 binding site, while the FITC group served as a signal reporter. By monitoring the interaction of F-TAK-875A with hGPR40-FLAG transfected HEK 293 cells, we established a FCM-based competitive binding assay to determine binding affinities of FFAs for hGPR40. With 18 saturated FFAs tested, we found that the binding potency of FFAs was clearly associated with their carbon chain lengths, in good agreement with previous findings measuring FFA agonist activity for hGPR40. Our molecular docking results showed that the binding pocket of the hGPR40 for TAK-875 could fully enclose FFAs with lengths shorter than C15, but not those with longer lengths. Our findings improve understanding of the pharmacological mechanism of action of FFAs on hGPR40 function.

Supporting Information

The Supporting Information is available free of charge on the ACS Publications website. 1 paragragh of text for fluorescence probe synthesis; scheme of synthesis of F-TAK-875A (Figure S1); HPLC analysis of F-TAK-875A (Figure S2); MS analysis of F-TAK-875A (Figure S3); NHR analysis of F-TAK-875A (Figure S4); effect of reaction time on the binding of F-TAK-875A to hGPR40 cells and FLAG cells (Figure S5); effect of the compounds on the non-specific binding of F-TAK-875A to FLAG cells at the highest tested concentration (Figure S6); effect of 1% DMSO on the binding of F-TAK-875A to hGPR40 cells (Figure S7); competitive binding results of TAK-875, GW9508, and 18 FFAs with hGPR40 (Figure S8); docking results of TAK-875, GW9508, and 18 FFAs with hGPR40 (Figure S9). Supporting materials may be accessed free of charge online at http://pubs.acs.org.

References

1. Kotarsky, K., Nilsson, N. E., Flodgren, E., Owman, C., and Olde, B. (2003) A human cell surface receptor activated by free fatty acids and thiazolidinedione drugs, *Biochem Biophys Res Commun 301*, 406-410.
2. Morgan, N. G., and Dhayal, S. (2009) G-protein coupled receptors mediating long chain fatty acid signalling in the pancreatic beta-cell, *Biochemical Pharmacology 78*, 1419-1427.
3. Huang, H., Dai, M. H., and Tao, Y. X. (2014) Physiology and therapeutics of the free fatty acid receptor GPR40, *Prog Mol Biol Transl Sci 121*, 67-94.
4. Milligan, G., Stoddart, L. A., and Brown, A. J. (2006) G protein-coupled receptors for free fatty acids, *Cellular Signalling 18*, 1360-1365.
5. Del Guerra, S., Bugliani, M., D'Aleo, V., Del Prato, S., Boggi, U., Mosca, F., Filipponi, F., and Lupi, R. (2010) G-protein-coupled receptor 40 (GPR40) expression and its regulation in human pancreatic islets: the role of type 2 diabetes and fatty acids, *Nutr Metab Cardiovasc Dis 20*, 22-25.
6. Ichimura, A., Hirasawa, A., Hara, T., and Tsujimoto, G. (2009) Free fatty acid receptors act as nutrient sensors to regulate energy homeostasis, *Prostaglandins Other Lipid Mediat 89*, 82-88.
7. Zhou, Y. J., Song, Y. L., Zhou, H., and Li, Y. (2012) Linoleic acid activates GPR40/FFA1 and phospholipase C to increase [Ca2+]i release and insulin secretion in islet beta-cells, *Chin Med Sci J 27*, 18-23.
8. Burant, C. F. (2013) Activation of GPR40 as a therapeutic target for the treatment of type 2 diabetes, *Diabetes Care 36*, S175-S179.
9. Tomita, T., Hosoda, K., Fujikura, J., Inagaki, N., and Nakao, K. (2014) The G-protein-coupled long-chain fatty acid receptor GPR40 and clucose metabolism, *Front Endocrinol 5*.
10. Feng, X. T., Leng, J., Xie, Z., Li, S. L., Zhao, W., and Tang, Q. L. (2012) GPR40: a therapeutic target for mediating insulin secretion (review), *Int J Mol Med 30*, 1261-1266.

11. Mancini, A. D., and Poitout, V. (2015) GPR40 agonists for the treatment of type 2 diabetes: life after 'TAKing' a hit, *Diabetes Obes Metab 17*, 622-629.

12. Christiansen, E., Urban, C., Merten, N., Liebscher, K., Karlsen, K. K., Hamacher, A., Spinrath, A., Bond, A. D., Drewke, C., Ullrich, S., Kassack, M. U., Kostenis, E., and Ulven, T. (2008) Discovery of potent and selective agonists for the free fatty acid receptor 1 (FFA(1)/GPR40), a potential target for the treatment of type II diabetes, *J Med Chem 51*, 7061-7064.

13. Yabuki, C., Komatsu, H., Tsujihata, Y., Maeda, R., Ito, R., Matsuda-Nagasumi, K., Sakuma, K., Miyawaki, K., Kikuchi, N., Takeuchi, K., Habata, Y., and Mori, M. (2013) A novel antidiabetic drug, fasiglifam/TAK-875, acts as an ago-allosteric modulator of FFAR1, *PLoS One 8*.

14. Negoro, N., Sasaki, S., Mikami, S., Ito, M., Suzuki, M., Tsujihata, Y., Ito, R., Harada, A., Takeuchi, K., Suzuki, N., Miyazaki, J., Santou, T., Odani, T., Kanzaki, N., Funami, M., Tanaka, T., Kogame, A., Matsunaga, S., Yasuma, T., and Momose, Y. (2010) Discovery of TAK-875: a potent, selective, and orally bioavailable GPR40 agonist, *ACS Med Chem Lett 1*, 290-294.

15. Briscoe, C. P., Peat, A. J., McKeown, S. C., Corbett, D. F., Goetz, A. S., Littleton, T. R., McCoy, D. C., Kenakin, T. P., Andrews, J. L., Ammala, C., Fornwald, J. A., Ignar, D. M., and Jenkinson, S. (2006) Pharmacological regulation of insulin secretion in MIN6 cells through the fatty acid receptor GPR40: identification of agonist and antagonist small molecules, *Br J Pharmacol 148*, 619-628.

16. Brown, S. P., Dransfield, P. J., Vimolratana, M., Jiao, X., Zhu, L., Pattaropong, V., Sun, Y., Liu, J., Luo, J., Zhang, J., Wong, S., Zhuang, R., Guo, Q., Li, F., Medina, J. C., Swaminath, G., Lin, D. C., and Houze, J. B. (2012) Discovery of AM-1638: a potent and orally bioavailable GPR40/FFA1 full agonist, *ACS Med Chem Lett 3*, 726-730.

17. Houze, J. B., Zhu, L., Sun, Y., Akerman, M., Qiu, W., Zhang, A. J., Sharma, R., Schmitt, M., Wang, Y., Liu, J., Medina, J. C., Reagan, J. D., Luo, J., Tonn, G.,

Zhang, J., Lu, J. Y., Chen, M., Lopez, E., Nguyen, K., Yang, L., Tang, L., Tian, H., Shuttleworth, S. J., and Lin, D. C. (2012) AMG 837: a potent, orally bioavailable GPR40 agonist, *Bioorg Med Chem Lett 22*, 1267-1270.

18. Defossa, E., and Wagner, M. (2014) Recent developments in the discovery of FFA1 receptor agonists as novel oral treatment for type 2 diabetes mellitus, *Bioorg Med Chem Lett 24*, 2991-3000.

19. Tan, C. P., Feng, Y., Zhou, Y. P., Eiermann, G. J., Petrov, A., Zhou, C., Lin, S., Salituro, G., Meinke, P., Mosley, R., Akiyama, T. E., Einstein, M., Kumar, S., Berger, J. P., Mills, S. G., Thornberry, N. A., Yang, L., and Howard, A. D. (2008) Selective small-molecule agonists of G protein-coupled receptor 40 promote glucose-dependent insulin secretion and reduce blood glucose in mice, *Diabetes 57*, 2211-2219.

20. Itoh, Y., Kawamata, Y., Harada, M., Kobayashi, M., Fujii, R., Fukusumi, S., Ogi, K., Hosoya, M., Tanaka, Y., Uejima, H., Tanaka, H., Maruyama, M., Satoh, R., Okubo, S., Kizawa, H., Komatsu, H., Matsumura, F., Noguchi, Y., Shinohara, T., Hinuma, S., Fujisawa, Y., and Fujino, M. (2003) Free fatty acids regulate insulin secretion from pancreatic beta cells through GPR40, *Nature 422*, 173-176.

21. Briscoe, C. P., Tadayyon, M., Andrews, J. L., Benson, W. G., Chambers, J. K., Eilert, M. M., Ellis, C., Elshourbagy, N. A., Goetz, A. S., Minnick, D. T., Murdock, P. R., Sauls, H. R., Jr., Shabon, U., Spinage, L. D., Strum, J. C., Szekeres, P. G., Tan, K. B., Way, J. M., Ignar, D. M., Wilson, S., and Muir, A. I. (2003) The orphan G protein-coupled receptor GPR40 is activated by medium and long chain fatty acids, *J Biol Chem 278*, 11303-11311.

22. Hara, T., Hirasawa, A., Sun, Q., Koshimizu, T. A., Itsubo, C., Sadakane, K., Awaji, T., and Tsujimoto, G. (2009) Flow cytometry-based binding assay for GPR40 (FFAR1; free fatty acid receptor 1), *Mol Pharmacol 75*, 85-91.

23. Lin, D. C., Guo, Q., Luo, J., Zhang, J., Nguyen, K., Chen, M., Tran, T., Dransfield, P. J., Brown, S. P., Houze, J., Vimolratana, M., Jiao, X. Y., Wang,

Y., Birdsall, N. J., and Swaminath, G. (2012) Identification and pharmacological characterization of multiple allosteric binding sites on the free fatty acid 1 receptor, *Mol Pharmacol 82*, 843-859.

24. Hauge, M., Vestmar, M. A., Husted, A. S., Ekberg, J. P., Wright, M. J., Di Salvo, J., Weinglass, A. B., Engelstoft, M. S., Madsen, A. N., Luckmann, M., Miller, M. W., Trujillo, M. E., Frimurer, T. M., Holst, B., Howard, A. D., and Schwartz, T. W. (2014) GPR40 (FFAR1) - Combined Gs and Gq signaling in vitro is associated with robust incretin secretagogue action ex vivo and in vivo, *Mol Metab 4*, 3-14.
25. Srivastava, A., Yano, J., Hirozane, Y., Kefala, G., Gruswitz, F., Snell, G., Lane, W., Ivetac, A., Aertgeerts, K., Nguyen, J., Jennings, A., and Okada, K. (2014) High-resolution structure of the human GPR40 receptor bound to allosteric agonist TAK-875, *Nature 513*, 124-127.
26. Negoro, N., Sasaki, S., Mikami, S., Ito, M., Tsujihata, Y., Ito, R., Suzuki, M., Takeuchi, K., Suzuki, N., Miyazaki, J., Santou, T., Odani, T., Kanzaki, N., Funami, M., Morohashi, A., Nonaka, M., Matsunaga, S., Yasuma, T., and Momose, Y. (2012) Optimization of (2,3-dihydro-1-benzofuran-3-yl)acetic acids: discovery of a non-free fatty acid-like, highly bioavailable G protein-coupled receptor 40/free fatty acid receptor 1 agonist as a glucose-dependent insulinotropic agent, *J Med Chem 55*, 3960-3974.
27. Schüttelkopf, A. W., and van Aalten, D. M. F. (2004) PRODRG: a tool for high-throughput crystallography of protein-ligand complexes, *Acta Crystallogr D60*, 1355-1363.
28. Tikhonova, I. G., and Poerio, E. (2015) Free fatty acid receptors: structural models and elucidation of ligand binding interactions, *BMC Struct Biol 15*, 015-0044.

Table 1. Highest concentration, IC_{50} values, RP and docking results for hGPR40 interactions with TAK-875, GW9508 and the 18 FFAs.

Compound	Highest concentration	IC_{50} (nM)	RP	Hydrogen binding
TAK-875	10 μM	3.1±0.8	1	Arg183,Tyr2240,Arg2258
GW9508	50 μM	25.1±2.8	0.12	Arg183,Arg2258
n-Caproic acid ($C_6H_{12}O_2$)	1 mM	ND[a]	ND	Arg183,Tyr2240,Arg2258
Heptanoic acid ($C_7H_{14}O_2$)	1 mM	ND	ND	Arg183,Tyr2240,Arg2258
Caprylic acid ($C_8H_{16}O_2$)	1 mM	>1000000[b]	ND	Arg183,Tyr2240,Arg2258
Nonanoic acid ($C_9H_{18}O_2$)	1 mM	1000000[b]	3.1×10^{-8}	Arg183,Arg2258
Capric acid ($C_{10}H_{20}O_2$)	1 mM	128435±51474	2.4×10^{-7}	Arg183,Tyr2240,Arg2258
Undecanoic acid ($C_{11}H_{22}O_2$)	1 mM	62946±9765	4.9×10^{-7}	Arg183,Arg2258
Lauric acid ($C_{12}H_{24}O_2$)	100 μM	8594±1296	3.6×10^{-6}	Arg183,Tyr2240,Arg2258
Tridecanoic acid ($C_{13}H_{26}O_2$)	100 μM	5126±595	6.1×10^{-4}	Arg183,Arg2258
Myristic acid ($C_{14}H_{28}O_2$)	30 μM	2409±786	1.3×10^{-3}	Arg183,Tyr2240,Arg2258
Pentadecanoic acid ($C_{15}H_{30}O_2$)	30 μM	1524±494	2.1×10^{-3}	Arg183,Arg2258
Palmitic acid ($C_{16}H_{32}O_2$)	30 μM	>30000[b]	ND	Arg183,Tyr2240,Arg2258
Heptadecanoic acid ($C_{17}H_{34}O_2$)	10 μM	ND	ND	Arg183,Arg2258
Stearic acid ($C_{18}H_{36}O_2$)	10 μM	ND	ND	Arg183,Tyr2240,Arg2258
Nonadecanoic acid ($C_{19}H_{38}O_2$)	10 μM	ND	ND	Arg183,Arg2258
Arachidic acid ($C_{20}H_{40}O_2$)	10 μM	ND	ND	Arg183,Arg2258
Heneicosanoic acid ($C_{21}H_{42}O_2$)	10 μM	ND	ND	Arg183,Tyr2240,Arg2258
Behenic acid ($C_{22}H_{44}O_2$)	10 μM	ND	ND	Arg183,Tyr2240,Arg2258
Tricosanoic acid ($C_{23}H_{46}O_2$)	10 μM	ND	ND	Arg183,Tyr2240,Arg2258

[a]ND = not determined

[b] IC50 values calculated by linear interpolation between two responses located around the 50% inhibition level.

Figure legends

Figure 1. Structures of compounds used in the experiments.

Figure 2. Expression of hGPR40 in HEK 293 cells. FCM analysis of FLAG transfected HEK 293 cells (A) and hGPR40-EGFP transfected HEK 293 cells (B).

Figure 3. Specific binding of F-TAK-875A to hGPR40. FCM analysis of FLAG and hGPR40 cell samples after incubation with 0, 10 and 100 nM F-TAK-875A (A); Comparison of the mean FITC signals of FLAG and hGPR40 cells after incubation with different concentrations of F-TAK-875A (B); Comparison of the histogram distribution of FITC signals of FLAG and hGPR40 cells after incubation with 100 nM F-TAK-875A, and FITC signals of hGPR40 cells after incubation with 100 nM F-TAK-875A and 10 μM TAK-875 (C); Determination of the percent of F-TAK-875A bound FLAG and hGPR40 cells after incubated with different concentrations of F-TAK-875A, and percent of FITC bound hGPR40 cells after incubated with different concentration of FITC (D). Experiments were conducted in triplicate and the data are means±SD. A p value of less than 0.05 was considered statistically significant.

Figure 4. Competitive binding curves of TAK-875, GW9508, n-caproic acid (C6), capric acid (C10), myristic acid (C14) and stearic acid (C18) on hGPR40. In the competitive binding assay, 50 μL hGPR40 cells, 100 nM F-TAK-875A and diluted test compounds were mixed in PBS at a total volume of 500 μL and incubated for 2 min at room temperature. The percentage of F-TAK-875A bound hGPR40 cells was plotted as a function of ligand concentration to obtain each competition curve. Experiments were conducted in triplicate and the data are means±SD.

Figure 5. Molecular docking results of hGPR40 interactions with TAK-875 (A), GW9508 (B), n-caproic acid (C), capric acid (D), myristic acid (E), stearic acid (F), pentadecanoic acid (G) and tricosanoic acid (H). In the docking results of A to F,

hGPR40 is represented in blue and ligands are in other colors. In the docking results of G and H, hGPR40 is represented in white and ligands are in red.

Figure 1.

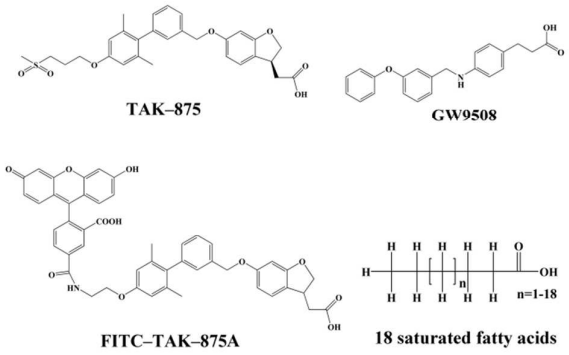

Figure 2.

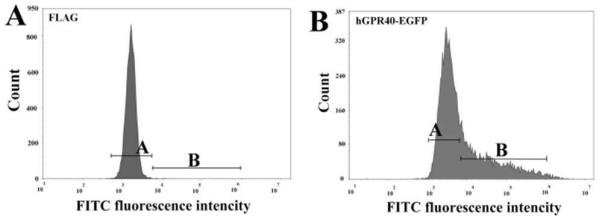
A
FLAG
Count
A
B
FITC fluorescence intencity
B
hGPR40-EGFP
Count
A
B
FITC fluorescence intencity

Figure 3.

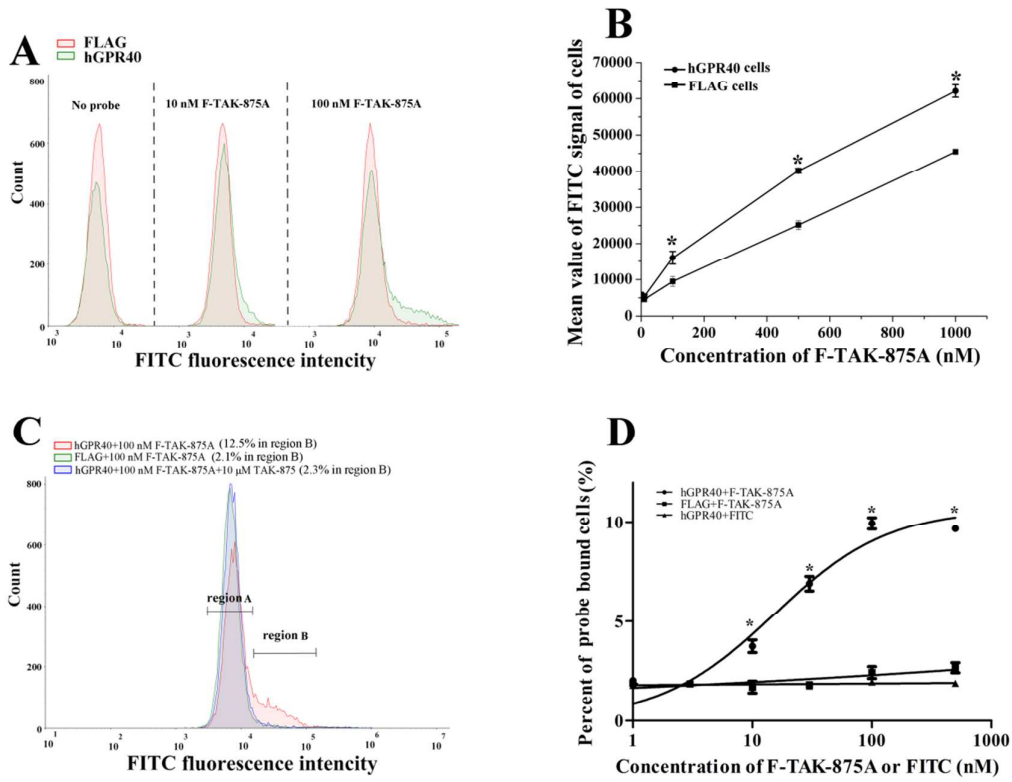
A
FLAG
hGPR40
No probe
10 nM F-TAK-875A
100 nM F-TAK-875A
Count
FITC fluorescence intencity
B
hGPR40 cells
FLAG cells
Mean value of FITC signal of cells
Concentration of F-TAK-875A (nM)
C
hGPR40+100 nM F-TAK-875A (12.5% in region B)
FLAG+100 nM F-TAK-875A (2.1% in region B)
hGPR40+100 nM F-TAK-875A+10 μM TAK-875 (2.3% in region B)
region A
region B
Count
FITC fluorescence intencity
D
hGPR40+F-TAK-875A
FLAG+F-TAK-875A
hGPR40+FITC
Percent of probe bound cells (%)
Concentration of F-TAK-875A or FITC (nM)

Figure 4.

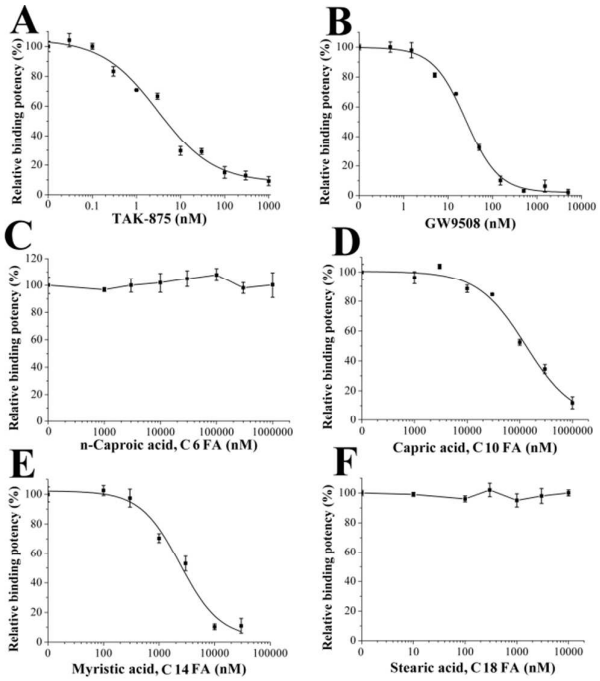
A
Relative binding potency (%)
TAK-875 (nM)
B
Relative binding potency (%)
GW9508 (nM)
C
Relative binding potency (%)
n-Caproic acid, C 6 FA (nM)
D
Relative binding potency (%)
Capric acid, C 10 FA (nM)
E
Relative binding potency (%)
Myristic acid, C 14 FA (nM)
F
Relative binding potency (%)
Stearic acid, C 18 FA (nM)

Figure 5.

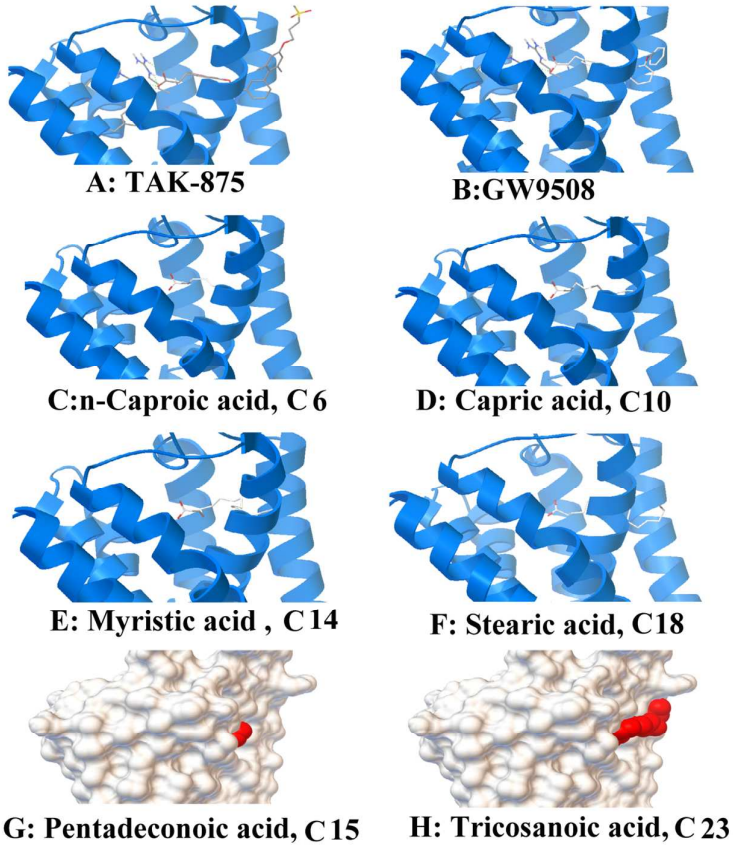
A: TAK-875
B:GW9508
C:n-Caproic acid, C 6
D: Capric acid, C10
E: Myristic acid , C 14
F: Stearic acid, C18
G: Pentadeconoic acid, C 15
H: Tricosanoic acid, C 23

Graphic for the Table of Contents:

For Table of Contents Use Only

Investigation of the binding interaction of fatty acids with human G protein coupled receptor 40 using a site-specific fluorescence probe by flow cytometry

Xiao-Min Ren[1], Lin-Ying Cao[1], Jing Zhang[1], Wei-Ping Qin[3], Yu Yang[1], Bin Wan[1], Liang-Hong Guo[1,2*]